JOURNAL OF APPLIED GEOSPATIAL INFORMATION

Vol 5 No 1 2021

http://jurnal.polibatam.ac.id/index.php/JAGI
ISSN Online: 2579-3608

The Tsunami Simulation Generated by 'Anak Krakatau' Volcano Flank Collapse using MIKE 21Hydrodynamics Flexible Mesh with Manning Number Variation

Hanah Khoirunnisa[1*], Wahyu Hendriyono[1], Mardi Wibowo[1]

[1)] Centre of Technology in Maritime Industrial Engineering, Indonesian Agency for the Assessment & Application of Technology (PTRIM - BPPT)

* Corresponding author email: hanah.khoirunnisa@bppt.go.id

Received: August 20, 2020
Accepted: February 17, 2021
Published: February 19, 2021

Abstract

This study aims to calculate the tsunami investment and the estimated arrival time at several locations around the Sunda strait, caused by the December 2018 Krakatao's eruption. The propagation of the tsunami wave is simulated using MIKE 21 Hydrodynamics Flexible Mesh (HD FM). The spatial data consist of the bathymetry and topography of the Sunda Strait area and its surroundings, whilst assumptions are made on the tsunami source topology and its exact location. Several runs of the simulation are then conducted by varying the Manning Number, i.e. bed resistance values, at the tsunami source and throughout the simulation domain, which accordingly would influence the propagation speed, inundation, and arrival time. Smaller Manning's values, which correspond to increasing roughness, are applied at locations closer to the tsunami source. In this simulation, Manning's number ranges from 10 to 40 $m^{1/3}s^{-1}$. Surface elevation, still water depth, and u and v velocity components are generated from this simulation.

Keywords: Flank Collapse, Manning numbers, MIKE 21 Hydrodynamics Flexible Mesh (HD FM), Tsunami Arrival Time

1. Introduction

On December 22, 2018 around 20.55 - 20.57 there was a tsunami in the Sunda Strait caused by the collapse of Mount Anak Krakatau. The collapse was caused by the eruption activity which began in June 2018 (Grilli et al., 2019). The Sunda Strait Tsunami is a volcanogenic tsunami, where the generation of the tsunami originates from volcanic activity. Volcanogenic tsunamis can be generated because of several things, namely volcanic eruptions in the sea, volcanic flow into the underwater, sudden collapse of volcanoes. These things can generate high amplitude sea waves, which are called volcanogenic tsunamis (Day, 2015 and Williams, et al., 2019). The Krakatau volcano tsunami that occurred on December 22, 2018 has caused the death of more than 400 people, and material losses in the surrounding areas, such as Serang, Ciwandan, Kota Agung, and Panjang Port (Williams, et al., 2019). Based on research conducted by Williams, et al (2019), it was found that the estimated volume of the Anak Krakatau mountain collapse was ~ 0.1 km3. In 2012, Giachetti et al conducted research on tsunamis caused by the collapse of the Mount Krakatau volcano. The majority of tsunami events that have occurred are caused by seismic, but there are some events caused by large volcanic eruptions, namely large lava flows entering seawater (de Lange. et al., 2001; Maeno and Imamura, 2007), underwater volcanic eruptions (Mader and Gitting, 2006). Based on research by Giachetti et al. (2012), the most probable cause of the tsunami is that the Mount Anak Krakatau is a collapsed mountain. Numerical modeling of tsunamis caused by the flank collapse of the Cumbre Vieja Volcano (La Palma, Canary Islands) volcano was carried out by Abadie, et al., (2012). In a study conducted by Abadie, et al., (2012), there were several scenarios of source volume from tsunamis. Luger, et al (2010) in his research have done tsunami modeling caused by earthquakes and underwater landslides using MIKE 21. Therefore, this research will discuss the propagation of tsunami waves and the arrival time of tsunamis caused by the collapse of children's mountains. Krakatau on December 22, 2018 with the influence of different manning.

2. Data and Methods

This tsunami wave propagation simulation is the result of hydrodynamic modeling using MIKE 21 software. The data used in this modeling are initial conditions of high sea level elevation at the point of

the flank collapse source, with a volume of 0.35 km3. In addition, field tidal data at the location where the tsunami occurred is also used. The data comes from the Geospatial Information Agency (BIG, 2018). The domain area to be simulated in this study is 178000 x 176000 m2 (Figure 1). The scenario used in this study is to apply manning variations in d in the simulation to be able to see the effect of the manning on the arrival time and height of the tsunami waves. Manning values applied in the study can be seen in Figure 4, namely 32 $m^{1/3}s^{-1}$ and 10 $m^{1/3}s^{-1}$, 15 $m^{1/3}s^{-1}$ and 10 $m^{1/3}s^{-1}$, 20 $m^{1/3}s^{-1}$ and 10 $m^{1/3}s^{-1}$, 10 $m^{1/3}s^{-1}$, and 5 $m^{1/3}s^{1}$.

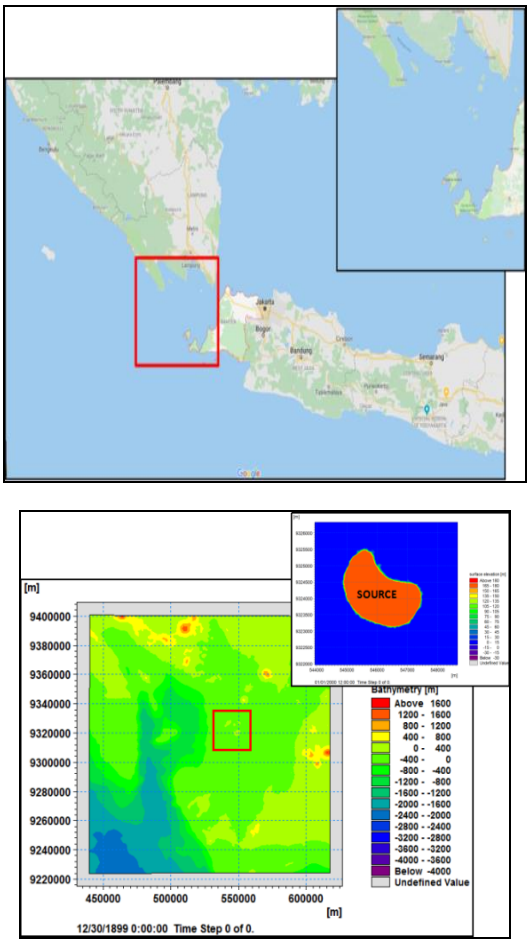

Fig 2. Domain and initial source condition of flank collapse tsunami of Mount Anak Krakatau simulation using MIKE 21.

Table 1. Extract point coordinate of the tsunami simulation result.

Location	Easting	Northing
Agung City	450000	9388000
Serang	590500	9315793
Ciwandan	605441	9337000
Pelabuhan Panjang	532900	9395325

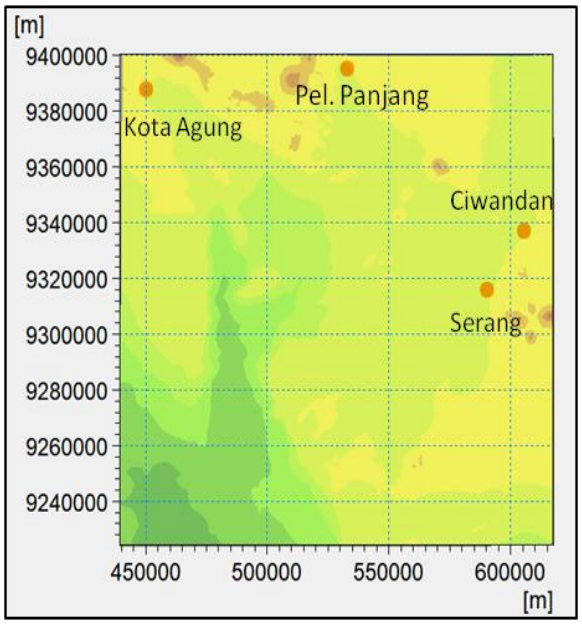

Fig 3. The extract points for the estimated arrival time and tsunami wave height result.

Fig 4 shows the condition of Mount Anak Krakatau for the years 2015 – 2019. The year of 2019's condition has already happened the tsunami. It appears that it is true that the collapse of Mount Anak Krakatau caused the tsunami. Below is an explanation of manning numbers. The seabed pressure force symbolized by is the result of the square of the law of friction, which is as below (DHI, 2011).

$$\frac{\overline{\tau_b}}{\rho_0} = c_f \overline{u_b}\left|\overline{u_b}\right|$$

Where *Cf* is the shear coefficient, $\overline{u_b}$ is the velocity above the seabed and ρ_0 is the density of water. For two-dimensional calculations, $\overline{u_b}$ is the velocity at the average depth and the shear coefficient can be determined from the Chezy number, C, or the manning number, M.

$$C_f = \frac{g}{C^2}$$

$$C_f = \frac{g}{(Mh^{1/6})^2}$$

Where h is the total depth of a waters and g is the acceleration due to gravity. The equation below is the relationship between the manning number and the length of the basic roughness.

$$M = \frac{25.4}{k_s^{1/6}}$$

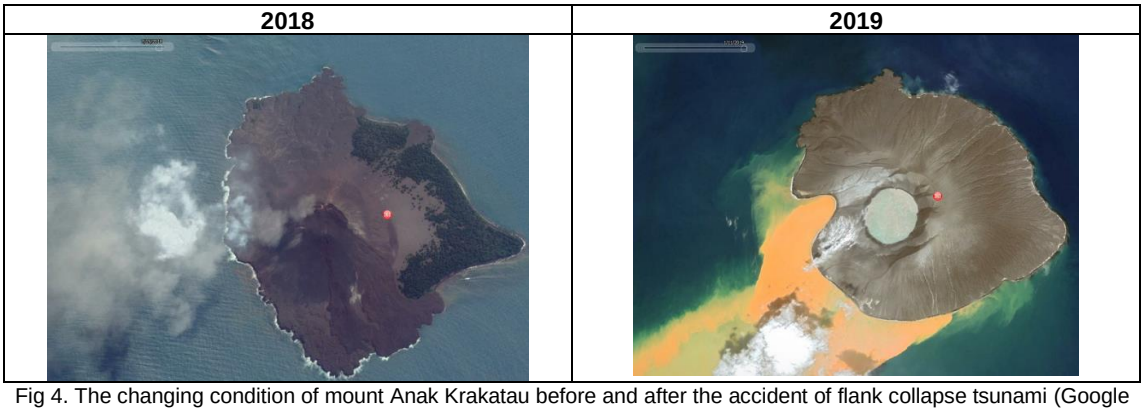

Fig 4. The changing condition of mount Anak Krakatau before and after the accident of flank collapse tsunami (Google earth, 2019).

3. Result and Discussion

Calculation of arrival time and height of tsunami elevation is done by using several bed roughness scenarios, where the manning values used are 32, 20, and 15 $m^{1/3}s^{-1}$ for all areas other than the source location, while the manning values for sources are used for values of 10. In addition, also used Manning values are constant for the entire area, ie 10 and 5. Based on the figure below, Serang has the highest tsunami height compared to other locations. Furthermore, Kota Agung has the second-largest maximum height after Serang, followed by Ciwandan and Pelabuhan Panjang. The figure below shows the wave propagation of the tsunami waves in the 15th, 30th and 45th minutes. It appears that the largest tsunami waves spread to the southeast charcoal, where the tsunami waves are directed towards the Banten area, and its surroundings with a maximum height of 1 m . While the volume used in this simulation is 0.35 km^3.

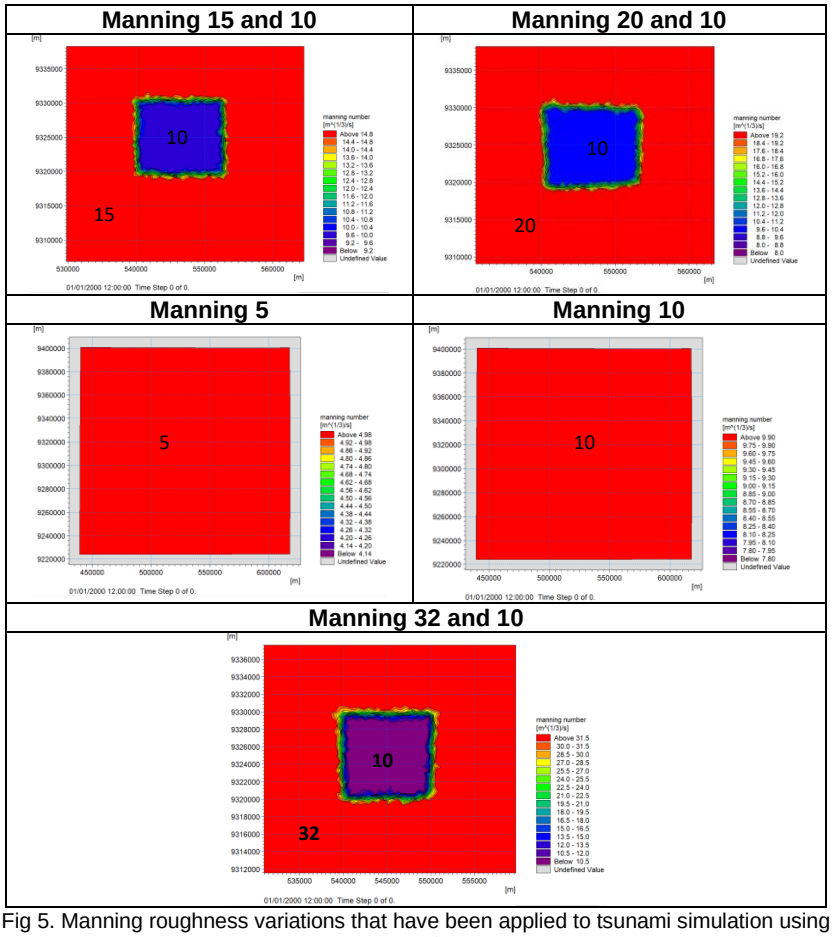

Fig 5. Manning roughness variations that have been applied to tsunami simulation using MIKE 21.

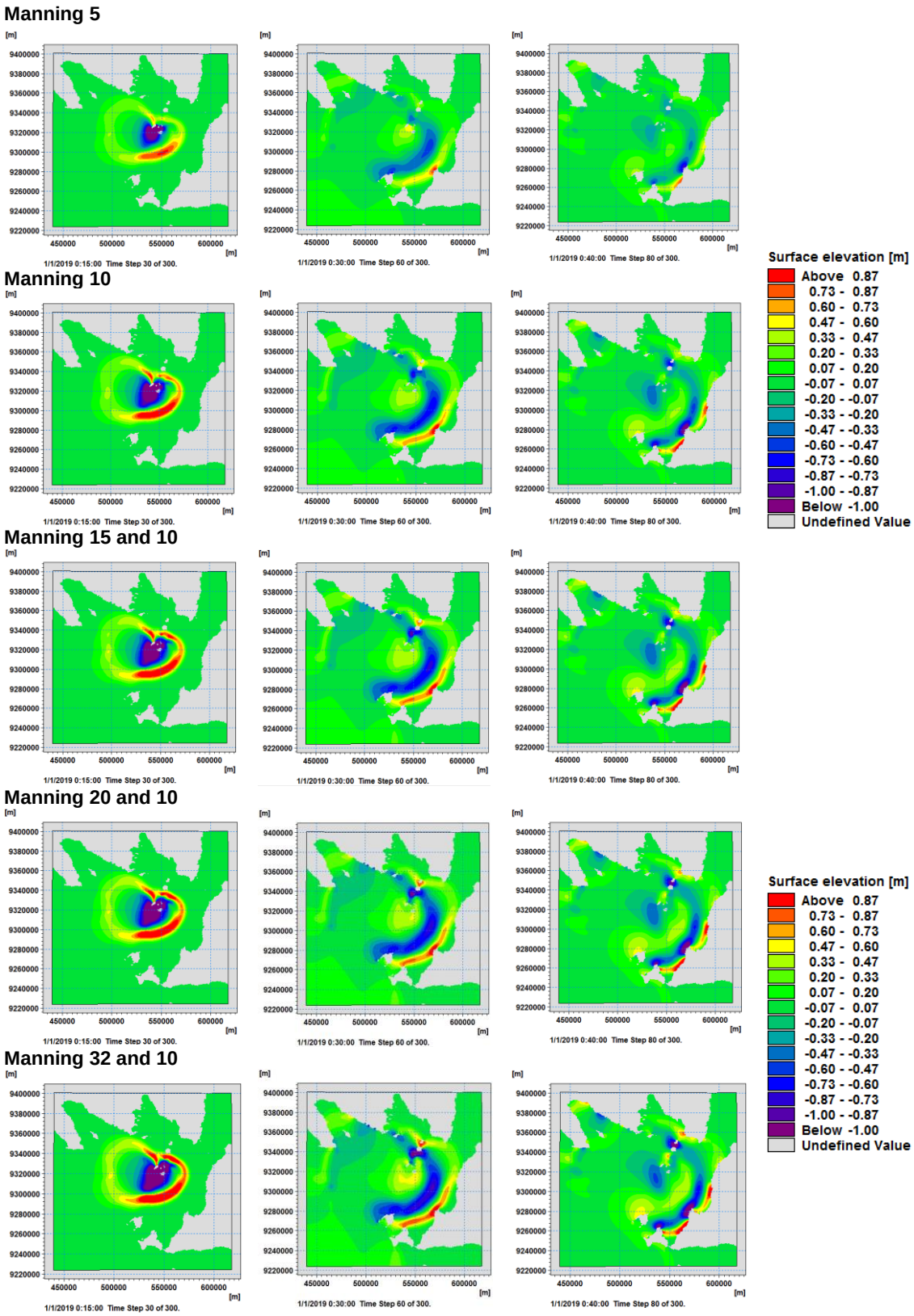

Fig 6. Tsunami wave propagation in domain area with several manning numbers for the time of 15, 30, and 40 minutes.

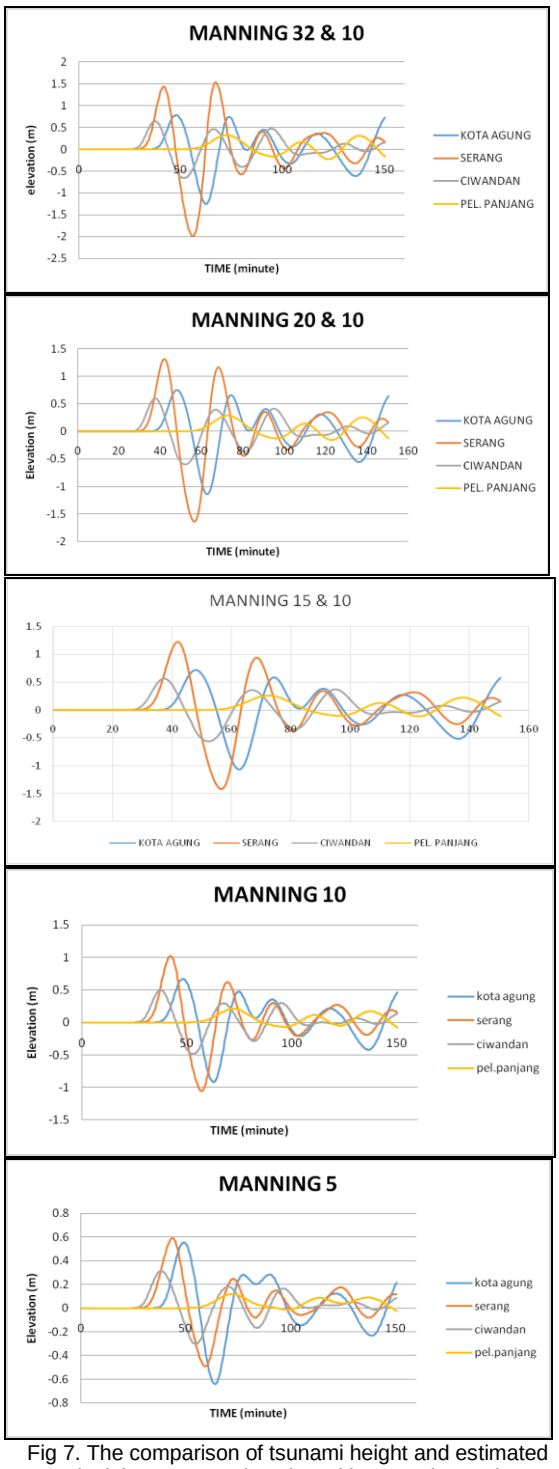

Fig 7. The comparison of tsunami height and estimated arrival time at every location with several manning numbers.

Table 2. Estimated arrival time tsunami at every location.

Location	Estimated arrival time (second)				
Agung City	37	37,5	37,5	37,5	37,5
Serang	30	30,5	30,5	30,5	31
Ciwandan	27	27,5	27,5	27,5	28
Panjang Port	55	56	56	56	57

Based on the estimated arrival time

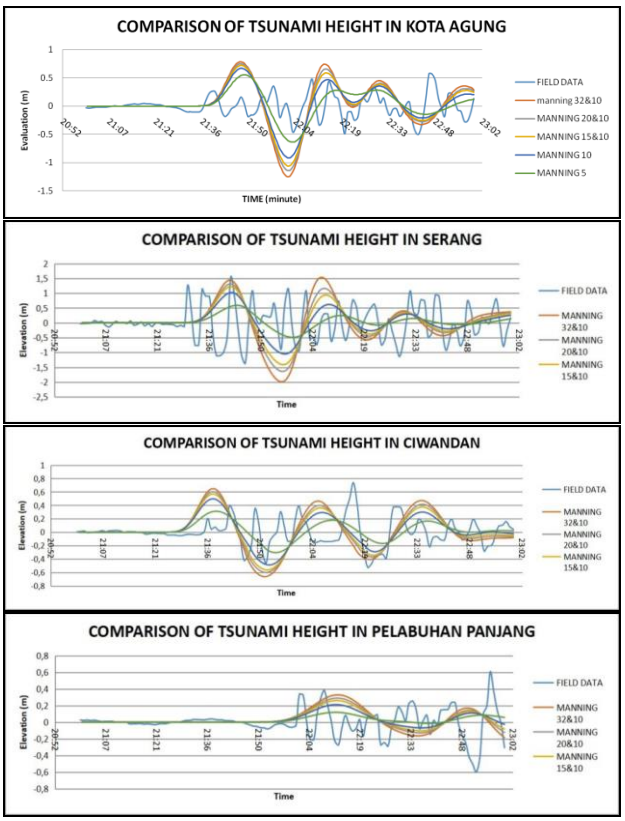

Fig 8. The affection of diversity of manning numbers for the estimated arrival time and tsunami height of each location.

Based on the Fig 8, it can be seen that the location of Agung City has the same height for every manning, except with a manning value of 5, where the yield of the tsunami height is lower than using other manning values for all locations. Based on the simulation results above, it can also be seen that the simulation results using MIKE 21 have a greater period when compared to the results of the field data. The comparison of the maximum, average, and minimum of the tsunami height at every manning can be seen on the table 3, 4, and 5.

Table 3. The maximum height of tsunamis in each city with various manning.

No	Location	Manning				
		32 & 10	20 & 10	15 & 10	10	5
1	Agung City	0,78	0,75	0,72	0,67	0,55
2	Serang	1,53	1,31	1,22	1,02	0,59
3	Ciwandan	0,65	0,60	0,57	0,50	0,31
4	Panjang Port	0,33	0,29	0,26	0,21	0,12

Table 4. The average height of tsunamis in each city with various manning.

No	Location	Manning				
		32 &10	20 & 10	15 & 10	10	5
1	Agung City	0,01	0,02	0,02	0,02	0,02
2	Serang	0,03	0,03	0,04	0,04	0,04
3	Ciwandan	0,02	0,02	0,02	0,02	0,02
4	Panjang Port	0,04	0,04	0,04	0,04	0,03

Table 5. The minimum height of tsunamis in each city with various manning.

No	Location	Manning				
		32 &10	20 & 10	15 & 10	10	5
1	Agung City	-1,25	-1,14	-1,06	-0,92	-0,64
2	Serang	-1,99	-1,64	-1,41	-1,05	-0,49
3	Ciwandan	-0,66	-0,60	-0,56	-0,49	-0,30
4	Panjang Port	-0,23	-0,16	-0,11	-0,08	-0,02

4. Conclusion

Based on the results of the study above, it can be seen that differences in the value of manning roughness can make different results to the height of tsunami waves in an area, but the difference is not significant. For the location of Kota Agung, the manning values of 32 and 10 caused the highest tsunami wave heights, namely 0.78. Likewise for the location of Serang, Ciwandan, and Panjang Port. For minimum low tide conditions, manning values 32 and 10 cause tsunami wave heights to have the lowest ebb in all locations. Based on the results of the simulation, it was also found that the arrival time for each location was different.

5. References

Abadie, S.M., Harris, J.C., Grilli, S.T. and Fabre, R., 2012. Numerical modeling of tsunami waves generated by the flank collapse of the Cumbre Vieja Volcano (La Palma, Canary Islands): tsunami source and near field effects. *Journal of Geophysical Research: Oceans*, *117*(C5).

Gayer, G., Leschka, S., Nöhren, I., Larsen, O. and Günther, H., 2010. Tsunami inundation modelling based on detailed roughness maps of densely populated areas. *Natural Hazards and Earth System Sciences*, *10*(8), p.1679.

Giachetti, T., Paris, R., Kelfoun, K. and Ontowirjo, B., 2012. Tsunami hazard related to a flank collapse of Anak Krakatau volcano, Sunda Strait, Indonesia. *Geological Society, London, Special Publications*, *361*(1), pp.79-90.

Grilli, S.T., Tappin, D.R., Carey, S., Watt, S.F., Ward, S.N., Grilli, A.R., Engwell, S.L., Zhang, C., Kirby, J.T., Schambach, L. and Muin, M., 2019. Modelling of the tsunami from the December 22, 2018 lateral collapse of Anak Krakatau volcano in the Sunda Straits, Indonesia. *Scientific reports*, *9*(1), pp.1-13.

Hasan, M.M., Rahman, S.M. and Mahamud, U., 2015. Numerical Modeling for the Propagation of Tsunami Wave and Corresponding Inundation. *IOSR J. Mech. Civil Eng*, *12*(2), pp.55-62.

Leschka, S., Pedersen, C. and Larsen, O., 2009, November. On the requirements for data and methods in tsunami inundation modelling–Roughness map and uncertainties. In *Proc. of the South China Sea Tsunami Workshop, Penang, Malaysia* (pp. 3-5).

Luger, S. and Harris, R.L., 2010, September. Modelling tsunami generated by earthquakes and submarine slumps using MIKE-21. In *International MIKE by DHI conference, South Africa, Paper* (p. P017).

Takabatake, T., Shibayama, T., Esteban, M., Achiari, H., Nurisman, N., Gelfi, M., Tarigan, T.A., Kencana, E.R., Fauzi, M.A.R., Panalaran, S. and Harnantyari, A.S., 2019. Field survey and evacuation behaviour during the 2018 Sunda Strait tsunami. *Coastal Engineering Journal*, pp.1-21.

Ward, S.N., 2001. Landslide tsunami. *Journal of Geophysical Research: Solid Earth*, *106*(B6), pp.11201-11215.

Williams, R., Rowley, P. and Garthwaite, M.C., 2019. Reconstructing the Anak Krakatau flank collapse that caused the December 2018 Indonesian tsunami. *Geology*, *47*(10), pp.973-976.

Williams, R., Rowley, P. and Garthwaite, M.C., 2019. Small flank failure of Anak Krakatau Volcano caused catastrophic December 2018 Indonesian tsunami.